Sodium inversion recovery MRI on the knee joint with an optimal inversion pulse

Jae-Seung Lee[1], Ding Xia[1], and Ravinder R. Regatte[1]
[1]*Department of Radiology, New York University, New York, NY, United States*

Target Audience: Scientists interested in sodium MRI and RF pulse design and clinicians in the field of cartilage imaging and
Purpose: In the field of sodium (^{23}Na) MRI, inversion recovery (IR) has been a popular method to discriminate the sodium content between different environments [1]. For cartilage imaging, IR can be used to suppress the signal from surrounding synovial fluid, which improves the sensitivity for the sodium content within cartilage *in vivo* [2]. While adiabatic pulses, such as WURST pulses [3], are usually used for the better inversion of the magnetization vector under B_0 and B_1 inhomogeneities, RF shapes robust against the field inhomogeneities can be obtained through numerical optimization based on optimal control theory (OCT) [4]. In this work, we designed optimal RF shapes to improve the performance of ^{23}Na IR MRI of the knee joint, in terms of fluid suppression, contrast between cartilage and artery, and specific absorption rate (SAR).
Method: (***Optimal inversion***) OCT was used to obtain RF shaped minimizing the z-component of the magnetization vector for the frequency offset from -1000 Hz to 1000 Hz and for the scaling of its RF amplitude from 80% to 120%, when applied to the initial thermal equilibrium magnetization. Its duration was set to be 10 ms, and its maximum RF amplitude (ω_1) was capped at $2\pi\times250$ Hz. The relaxation times T_1 and T_2 were assumed to be same and set to be 43 ms. (***^{23}Na knee MRI***) The right knee joint of one healthy volunteer was scanned on a 7T Siemens scanner with an in-house custom built double-tuned knee coil (8ch-^{23}Na/4ch-^{1}H). Sodium images were acquired with Fermat looped, orthogonally encoded trajectories (FLORET [5]) consisting of 3 hubs at 45°, each of which comprises 332 interleaves. The parameters for the image acquisition were FOV = (220 mm)^3, TE = 0.2 ms, TR = 140 ms, Nyquist resolution = 3.4 mm, ADC duration = 6.6 ms, 8 averages, the flip angle/duration of the excitation pulse = 80°/0.6 ms, and the total acquisition time = 16:36. Standard 3D regridding was used to reconstruct the images with a nominal resolution of 2 mm. Fluid suppressions were performed using inversion recovery with an optimal pulse and the WURST-20 pulse [3]. For the optimal pulse, the inversion time (TI) was 26 ms. For the WURST-20 pulse, the duration, amplitude, and TI were 10 ms, 240 Hz, and 24 ms.
Results: (***Optimal inversion***) The waveform and performance of the WURST-20 pulse and an optimal inversion pulse were presented in Fig. 1. The inversion efficiency of the optimal pulse was higher by 13% while the RF power should be smaller by 38%. Moreover, the optimal pulse manifests more symmetrical performance with respect to the frequency offset and RF amplitude scaling (Fig. 1c vs. Fig. 1d). (***^{23}Na knee MRI***) Figure 2 shows slices from ^{23}Na images acquired without IR, with IR using the WURST-20 pulse shown in Fig. 1a, and with IR using the optimal pulse shown in Fig. 1b.
Discussion: By replacing the WURST-20 pulse with the optimal inversion pulse, the SNR from cartilage tissues increased by 4 – 18%, and SAR was reduced by almost 50%. However, the signal from an artery was not suppressed as much, probably because the T_1 of sodium content in blood is shorter than the T_1 used in the numerical optimization. Another possibility is that the optimal inversion pulse might be less sensitive to the variation of T_1 than the WURST-20 pulse.
Conclusion: Based on OCT, an inversion pulse was designed and implemented on 7T to improve the performance of ^{23}Na IR MRI. In this preliminary work, an optimal inversion pulse demonstrated its potential for ^{23}Na IR MRI on the knee joint.

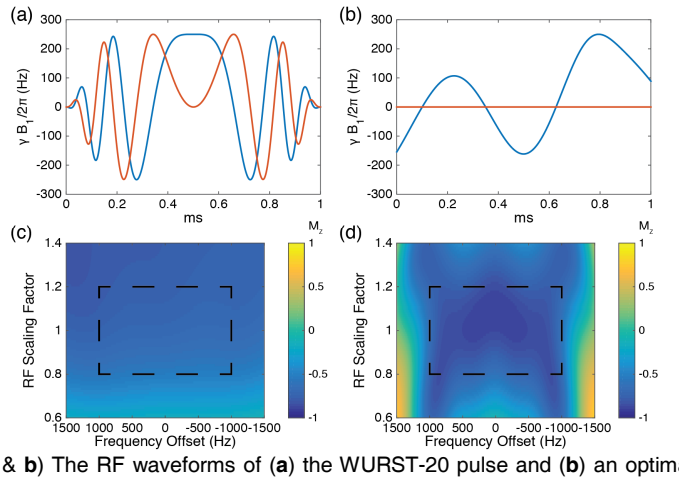

Fig. 1 (**a** & **b**) The RF waveforms of (**a**) the WURST-20 pulse and (**b**) an optimal pulse. The blue (red) line represent the *x* (*y*) component of RF. (**c** & **d**) The *z* components of the magnetization vector after applying (**c**) the WURST-20 pulse and (**d**) the optimal pulses to the initial thermal equilibrium state ($M_x = M_y = 0$, $M_z = 1$). The black dashed box shows the ranges of the frequency offset and RF scaling used in the numerical optimization.

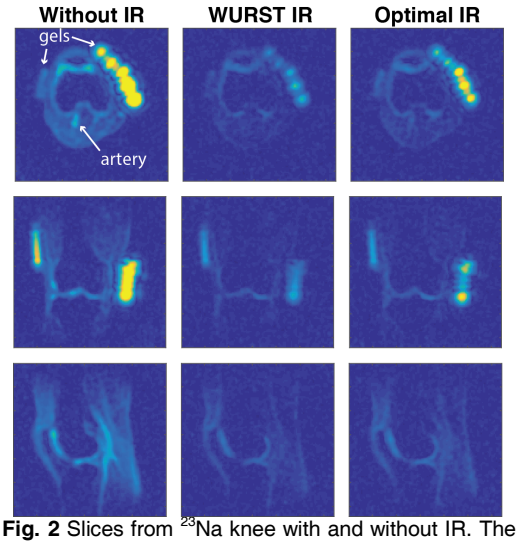

Fig. 2 Slices from ^{23}Na knee with and without IR. The WURST-20 and optimal pulses shown in Fig. 1 were used respectively for 'WURST IR' and 'Optimal IR'.

References: [1] Madelin G, Lee J-S, Regatte RR, Jerschow A. Prog. NMR Spectrosc. 2014;79:14. [2] Madelin G, Babb J, Xia D, Chang G, Krasnokutsky S, Abramson SB, et al. Radiology. 2013;268:481. [3] Kupče Ē, Freeman R. J. Magn. Reson. 1995;115:273. [4] Lee J-S, Regatte RR, Jerschow A. Chem. Phys. Lett. 2010;494:331. [5] Pipe JG, Zwart NR, Aboussouan EA, Robison RK, Devaraj A, Johnson KO. Magn. Reson. Med. 2011;66:1303.